Phase Behavior of Mixtures of Rods (Tobacco Mosaic Virus) and Spheres (Polyethylene Oxide, Bovine Serum Albumin)

Marie Adams and Seth Fraden
Martin Fisher School of Physics, Brandeis University, Waltham, Massachusetts 02254 USA

ABSTRACT Aqueous suspensions of mixtures of the rodlike virus tobacco mosaic virus (TMV) with globular macromolecules such as polyethylene oxide (PEO) or bovine serum albumin (BSA) phase separate and exhibit rich and strikingly similar phase behavior. Isotropic, nematic, lamellar, and crystalline phases are observed as a function of the concentration of the constituents and ionic strength. The observed phase behavior is considered to arise from attractions between the two particles induced by the presence of BSA or PEO. For the TMV/BSA mixtures, the BSA adsorbs to the TMV and bridging of the BSA between TMV produces the attractions. For TMV/PEO mixtures, attractions are entropically driven via excluded volume effects known alternatively as the "depletion interaction" or "macromolecular crowding."

DEDICATION

Don Caspar first introduced me (SF) to the fascinating properties of suspensions of tobacco mosaic virus (TMV) in 1980, and I have been studying their liquid crystalline and colloidal properties ever since. Although Prof. Caspar is principally known as a structural biologist, and for his contributions to the elucidation of intramolecular structure, he has had a long interest in interparticle structure and collective organization. The goal of the work presented here is to understand the physical basis of polymer-induced crystallization of proteins, a problem of great importance to x-ray crystallography and in understanding the compartmentalization of DNA and other filamentous molecules in cytoplasm. Not surprisingly, Prof. Caspar has worked on this problem in the past, and a poster containing several of the results presented below hung on the walls of his laboratory at Brandeis for many years. Not uncharacteristically, Prof. Caspar's work has gone unpublished, perhaps because all of the questions posed by the observations were not answered thoroughly enough for Don's standards. Our work presented here is far from complete. The problem of polymer-induced phase separation has been studied independently by physicists, chemists, and biologists. Often the work of one discipline is unknown to others. It is the objective of this paper to study this problem experimentally, using well-characterized model systems, and to analyze the observations within the framework of theories known as "depletion interaction" or "macromolecular crowding."

INTRODUCTION

The concept that entropy alone is sufficient to drive a transition from a disordered to ordered phase is an old one in colloidal science (Onsager, 1949; Israelachvili and Ninham, 1977; Forsyth et al., 1978; Flory, 1978; Frenkel, 1993). Most colloidal suspensions consist of particles whose interactions are dominated by steric repulsion (that is no two particles can occupy the same place simultaneously), and so it is natural to consider the simplified case of hard particles as a model system. Once the properties of this model system are understood, more realistic models can be constructed by adding the other relevant interactions in a perturbative manner.

The phase behavior of a colloidal suspension of hard particles is found by minimizing the free energy $F = U - TS$, where the interaction energy U is zero for steric particles. Thus the phase behavior of hard particles is determined by maximizing the entropy S. Examples of entropically driven ordering are the liquid crystalline phases exhibited by hard rods such as the isotropic, nematic, smectic, columnar, and crystalline phases, or the fluid-crystal transition of hard spheres. These phase transitions have been studied extensively with theory (Onsager, 1949; Odijk, 1986; Semenov and Khokhlov, 1988; Vroege and Lekkerkerker, 1992) and computer simulations (Frenkel, 1991) and experimentally in a variety of colloidal systems, including tobacco mosaic virus (Onsager, 1949; Wetter, 1985; Meyer, 1990; Wang et al., 1994; Fraden, 1995). Another class of entropically driven ordering arises in mixtures where demixing transitions are often observed to occur. The usual scenario is that if the shape of the two components is different enough, bulk phase separation will occur for an appropriate composition of the components.

The physical origin of the entropically driven phase transitions in colloidal mixtures is both extremely simple and general. The free volume of a suspension composed of a binary mixture of macromolecules is maximized when the two components phase separate. Increasing the free volume (or reducing excluded volume) raises the translational entropy of the macromolecules, but at the expense of lowering the entropy of mixing. At low concentrations, the mixing entropy dominates and the solution is miscible, but with

Received for publication 28 May 1997 and in final form 18 August 1997.
Address reprint requests to Marie Adams, Physics Department, Mail Stop 057, Brandeis University, Waltham, MA 02254-9110. Tel.: 617-736-2877; Fax: 617-736-2915; E-mail: marie@smectic.elsie.brandeis.edu.

0006-3495/98/01/669/09 $2.00

increasing concentration, if the gain in free volume is sufficient, phase separation will occur. This effect is known by several different names. It is called the *depletion effect* in physics and chemistry (Asakura and Oosawa, 1958; Flory, 1978; Gast et al., 1986; Mahadevan, 1990; Bolhuis and Frenkel, 1994; Lekkerkerker and Stroobants, 1994; Lekkerkerker et al., 1995), but is known as *macromolecular crowding* in biology (Walter and Brooks, 1995; Minton, 1995; Herzfeld, 1996). The depletion effect may drive like particles to flocculate (depletion attraction), or in some cases may account for an effective repulsion between them (depletion repulsion) (Mao et al., 1995; Walz and Sharma, 1994; Sober and Walz, 1995).

There are compelling arguments for expecting this effect to be important in the biological problem known as microcompartmentalization (Walter and Brooks, 1995; Welch and Clegg, 1986). This refers to the observation that macromolecules in the cell are not uniformly distributed, but tend to segregate. In particular, biopolymers, such as DNA, actin, and microtubules, are often observed to bundle together into fibers. Macromolecules occupy 30% of the volume of the cell, strongly influencing intermolecular interactions. Even in the absence of any direct interactions between particles, such as electrostatic, hydrophobic, or van der Waals forces, the macromolecules feel each others' presence simply because two molecules cannot occupy the same place at the same time. Reducing excluded volume causes like species to phase separate into different regions of the cell, leading to macromolecular compartmentalization without the need for any intracellular membranes, as observed for DNA in prokaryotes.

The biochemistry of the cell has evolved in a thermodynamically nonideal environment, with high intracellular macromolecular concentrations, and it may be that the cell has exploited this fact. Long, hard filaments alone in suspension will remain dispersed because of the entropy of mixing, but when globular macromolecules at typical intracellular concentrations are added to the suspension, the filaments will phase separate into rod-rich and rod-poor regions (Suzuki et al., 1989; Cuneo et al., 1992). For certain conditions, the demixing is complete and the rods close-pack into bundles. Bundling could be important in the phenomena of protoplasmic streaming, a form of locomotion in single cells where actin filaments assemble in the region of the cell that is moving forward. One can imagine that the cell takes advantage of the depletion forces to assemble filaments into fibers, rather than expending energy to construct and regulate specific proteins to do the job. However, it is well known that specific actin-bundling proteins do exist. It could be that the role of specific bundling proteins is to fine-tune certain aspects of the fiber assembly, such as providing a polar alignment of the bundled biopolymers. Spontaneous bundling due to macromolecular crowding has also been implicated in sickle-cell hemoglobin fiber formation (Herzfeld, 1996), and in cytoskeletal organization (Walter and Brooks, 1995). Although several studies have been made of poly(ethylene glycol) (PEG)-induced bundling of actin filaments, detailed comparison of the experimental data with existing statistical mechanical theories still remains to be done (Suzuki et al., 1989; Cuneo et al., 1992). It is interesting to note that the biological community interested in macromolecular crowding (Walter and Brooks, 1995; Minton, 1995; Herzfeld, 1996; Welch and Clegg, 1986; Suzuki et al., 1989; Cuneo et al., 1992) seems unaware of the extensive theories developed by the chemical/physics community (Asakura and Oosawa, 1958; Flory, 1978; Gast et al., 1986; Bolhuis and Frenkel, 1994; Lekkerkerker and Stroobants, 1994; Lekkerkerker et al., 1995).

A second area of biological importance is the question of protein crystallization induced by the addition of a nonadsorbing polymer. This is an old technique, but only in the last several years has there been an attempt at theoretical modeling of the interactions responsible for crystallization (Mahadevan, 1990; Smits et al., 1992; Rosenbaum et al., 1996; Asherie et al., 1996; Poon, 1997). Clearly, a thorough understanding of this phenomenon will lead to improved methods of inducing protein crystallization, an important part of structural biology.

MATERIALS

It is the objective of this paper to qualitatively describe the observed phase behavior of mixtures of rodlike biopolymers and globular macromolecules to ascertain if the current theoretical models are applicable to model experimental systems. In particular, we wanted to use a biopolymer that exhibited a range of liquid crystalline phases (isotropic, nematic, smectic, crystalline), and for this study we choose tobacco mosaic virus (TMV). Unfortunately, the TMV stock we used, although initially monodisperse, had become polydisperse with age, resulting in the suppression of the smectic and colloidal crystalline phases for the pure virus suspensions. For a globular macromolecule we used either bovine serum albumin (BSA), a compact protein, or polyethylene oxide (PEO), a Gaussian-coiled water-soluble polymer.

All of the samples were in 50 mM sodium borate buffer (ionic strength 7 mM) with a pH of 8.5. TMV is a rodlike virus 300 nm in length and 18 nm in diameter (D). TMV is charged, and two TMV particles will repel each other. An effective diameter (D_{eff}), larger than the physical diameter D, can be calculated from the free energy (Onsager, 1949; Stroobants et al., 1986). Loosely speaking, D_{eff} is the distance of separation of two rods for which the potential energy of repulsion is equal to the thermal energy when averaged over the angular distribution of the rods. Thus TMV can be modeled as a hard rod with an increased effective diameter, which for this buffer is ~35 nm (Fraden et al., 1993).

The TMV was mixed with two different spherical colloids, a coiled polymer and a globular protein. The coiled polymer used in this study was polyethylene oxide, molecular weight 100,000, corresponding to a radius of gyration of ~10 nm (Devanand and Selser, 1990). The polymer is commercially available as a powder (Aldrich, Milwaukee, WI; Fluka, Ronkonkoma, NY) and can be added directly to the buffer solution. The solubility of PEO 100,000 seemed to be limited to ~60 mg/ml. The globular protein used in the mixtures was bovine serum albumin (BSA). This protein has a hydrodynamic radius of ~3.7 nm (Ullmann et al., 1985). BSA is commercially available as a solid (Sigma, St. Louis, MO), which can be dissolved in the buffer. A solution of 100 mg/ml BSA was made as a stock solution for this study.

Analytical centrifuge measurements of the TMV stock suspension used in this study revealed the virus to be polydisperse: ~20% by weight of end-to-end aggregated dimer particles of length 600 nm with 80% by weight monomer particles. Below 75 mg/ml, the TMV suspension is isotropic, and the isotropic-nematic coexistence ranges from ~75 mg/ml to

200 mg/ml. The polydispersity of the sample accounts for the large isotropic-nematic coexistence region observed in samples made of the pure rod system (Fraden et al., 1993; Vroege and Lekkerkerker, 1993). Concentrations greater than 200 mg/ml appear to be a single nematic phase, but with weak thermal fluctuations of the nematic director, typical of aggregated samples.

The concentration of TMV was determined by measuring UV absorption with a Beckman spectrophotometer (Beckman Instruments, Columbia, MD). The extinction coefficient used was an optical density of 3.06 measured at 265 nm, for a 1-cm path length, and for a 1 mg/ml solution.

METHODS

Our evaluation of the TMV mixtures has been qualitative. Sample behavior has been classified by using optical microscopy observations at both high and low magnifications. A range of TMV concentrations and a range of polymer concentrations used in this study form a concentration space. Multiple samples have been prepared that span this space. Those samples exhibiting the same general features are grouped together to define a region of concentration space. The samples have been categorized into several such regions. The boundaries of these regions are defined by notable distinctions in birefringence, features of observed texture, density of texture, dynamics, and surface and bulk behavior of the sample.

The microscope used was a Nikon Microphot-SA equipped with a 60× DIC NA 1.4 objective and condensor (Nikon Corporation, Tokyo, Japan). The light source was a 100-W quartz lamp. The images were acquired with a Scion frame grabber (Scion Corporation, Frederick, MD) on a Power Macintosh 8500/120 computer (Apple Computer, Cupertino, CA) running National Institutes of Health Image (developed at the U.S. National Institutes of Health and available on the internet at http://rsb.info.nih.gov/National Institutes of Health-image/). The only video processing was the adjustment of brightness and contrast.

RESULTS

Observations: mixtures of TMV and either BSA or PEO 100,000

A sample may have characteristic features. It may appear to have a single texture throughout, or alternatively, discrete formations of various size, shape, and birefringence may be observed within the sample. Pure TMV suspensions exhibit liquid crystal phases above a critical density (which increases with increasing ionic strength). In the liquid crystal phases, the rod axes align roughly parallel to one another and the suspension becomes optically birefringent, whereas dilute suspensions are optically isotropic. Monodisperse nematic TMV suspensions have large thermally excited fluctuations of the director, which scatter and depolarize light. These fluctuations are greatly suppressed in the aggregated samples.

The textures of the TMV mixtures may appear viscous and dense, or may appear to flow more freely. In general, the more viscous samples appear largely static with features frozen in place, and the thermal fluctuations of the director are absent as well. For the more fluid samples, we can look at the dynamics of the structures formed within those samples to make distinctions between different regions. In some samples, droplet structures form that are highly birefringent and appear to have violent internal fluctuations. Yet, in other samples, a highly birefringent precipitate forms that exhibits essentially no visible internal fluctuations. In this case, the dynamics of these structures separates two distinct regions of concentration space. X-ray studies need to be performed to ascertain the state of these condensed structures. We speculate that the dynamic condensates are a liquid phase and that the static condensates are crystalline.

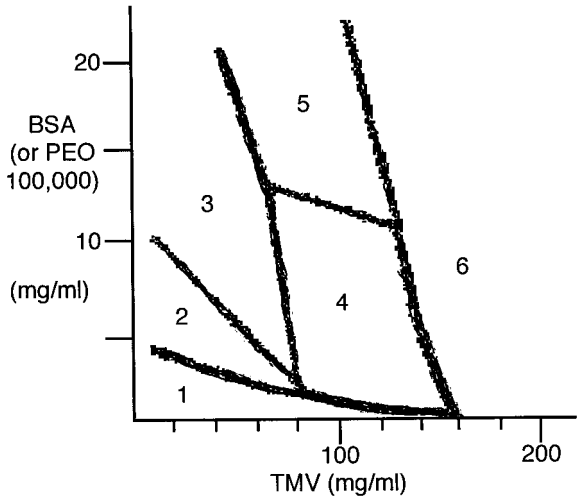

FIGURE 1 Concentration space for TMV and BSA/PEO 100,000. This diagram indicates the six regions used to categorize our samples. The buffer was 50 mM sodium borate buffer at pH 8.5 and had an ionic strength of 7 mM. The phase sequence of pure TMV was isotropic below 75 mg/ml, isotropic-nematic coexistence between 75 mg/ml and 200 mg/ml, and a single nematic phase above 200 mg/ml.

Our observations for the TMV and BSA mixed system and for the TMV and PEO 100,000 mixed system are almost identical. Because of this, in the descriptions that follow, the word "depletant" is used to refer to either BSA or PEO 100,000. In some cases, BSA or PEO 100,000 is explicitly indicated. The concentration regions investigated are repre-

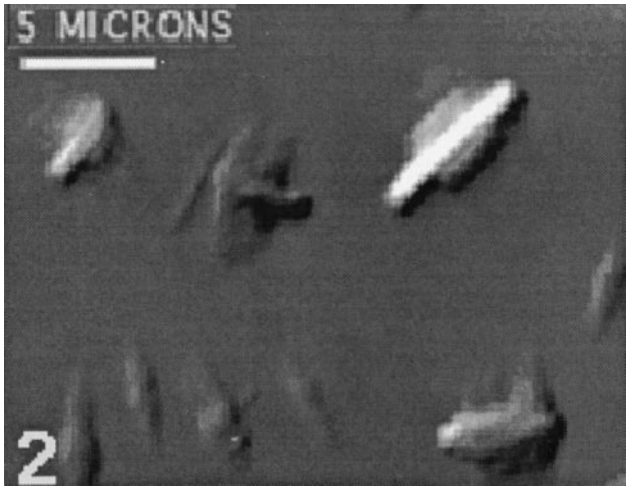

FIGURE 2 20 mg/ml TMV; 8 mg/ml BSA. The sample corresponds to region 2 of the concentration space. Amorphous droplets of low birefringence and rodlike droplets of high birefringence are observed. The droplets exhibited violent thermal fluctuations. The photograph was taken within the bulk of the sample, using high-magnification differential interference microscopy.

sented in a schematic diagram shown in Fig. 1. This diagram is broken up into six regions, each representing an area of sample space that exhibited a distinct morphology. Some regions do define areas of real phase separation; however, other regions are distinguished by differences in viscosity, or in size of domains.

Regions 1, 2, and 3 are areas with low concentrations of TMV (isotropic in a pure rod suspension). As depletant is added to the pure TMV system of low concentration, it is initially isotropic and miscible (region 1). As more depletant is added, the mixture begins to exhibit evidence of flocculation (region 2). In region 2, we observe an isotropic liquid phase in which droplet-like structures take form (Fig. 2). In the first stages of formation, the droplets are very faint, and do not appear to be appreciably birefringent when viewed under crossed polarizers. These structures take on a variety of shapes; many of them are amorphous droplets with rodlike growths. Others are more oblong and seedlike in shape. Still others are distinctly rod-shaped, and these appear more birefringent than the other droplets. All of these structures have a tendency to stick together, as in the observed stacking of two or three seed objects or the coalescence of a few droplets (Fig. 2). The droplets are extremely dynamic and fluctuate violently, such that the droplet boundary undulates. As the depletant concentration continues to increase, the boundaries of the droplets become more clearly defined and the shapes of the droplets become less varied.

As the droplets transform into more macroscopic rodlike shapes, we cross the boundary into region 3 (Fig. 3, *a* and *b*). Region 3 corresponds to TMV concentrations which, for the pure rod system, range from the isotropic to very close to the transition between isotropic behavior and isotropic-nematic coexistence. For samples of depletant within region 3 mixed with the TMV concentration just near this transition, we again note an isotropic liquid phase (*black under crossed polarizers* in Fig. 3 *b*) in which macroscopic objects begin to take form (*white*, indicating birefringence, in Fig. 3 *b*). Well-defined rodlike structures mixed with hexagonal or round plates are observed in Fig. 3 *c*. These rods and plates are a more developed stage of those droplets formed in region 2.

These rods have been observed in a range of sizes. Some are more rounded in shape, whereas others are distinctly rectangular. Widths range from ~0.7 μm to 3 μm. The formation of these macroscopic rods indicates a phase separation. The rod's shape is qualitatively different from that observed in other immiscible liquids. More commonly in

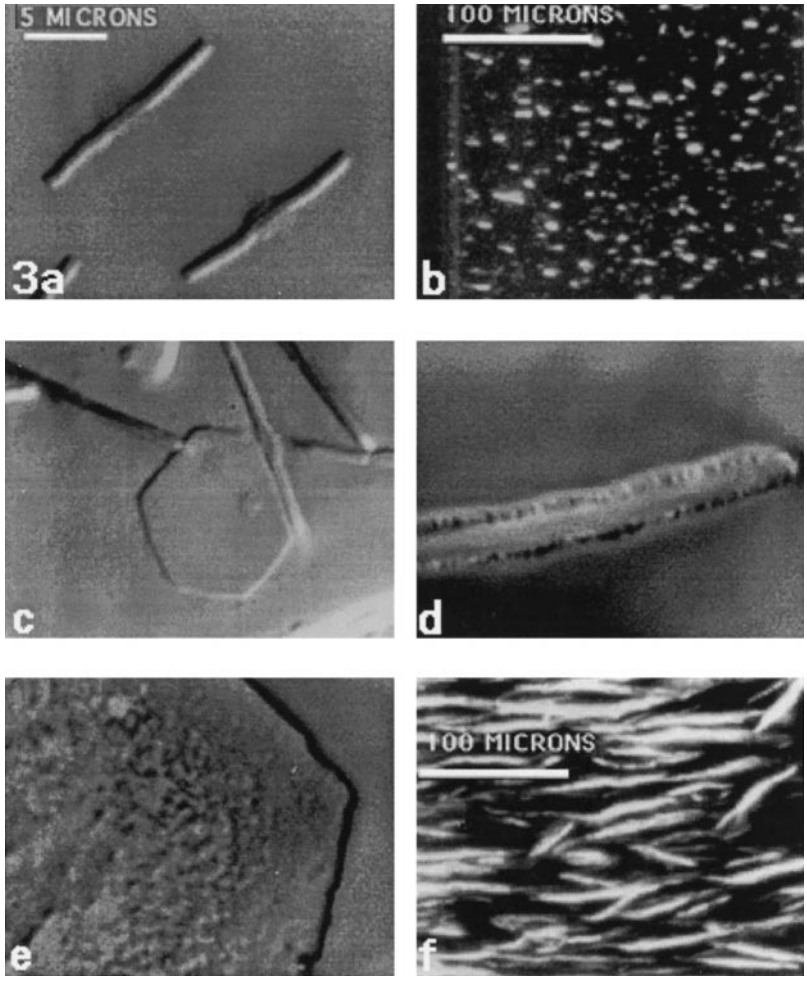

FIGURE 3 These samples correspond to behavior observed in region 3 of concentration space. Samples *a*, *c*, *d*, and *e* are at high magnification; samples *b* and *f* are at low magnification. (*Samples a* and *b*) 32 mg/ml TMV; 20 mg/ml BSA. The formation of macroscopic rods in an isotropic liquid phase was observed in this sample under high magnification (*a*) and low magnification (*b*). (*Sample c*) 16 mg/ml TMV; 8 mg/ml PEO 100,000. The coexistence of macroscopic rods and hexagonal plates was observed. (*Samples d* and *e*): 75 mg/ml TMV; 7 mg/ml PEO 100,000. Rods in this sample exhibit debris along the perimeter (*d*), whereas the hexagonal plates in this same sample have a notable surface texture (*e*). This is the same sample as in *a* and *b*, having evolved with time into much longer rodlike structures (*f*). All of the above photographs were taken within the bulk of the samples. High-magnification photographs are differential interference microscopy. Low-magnification photographs are standard polarization microscopy.

liquid/liquid mixtures, round or ellipsoidal droplets are observed. Two immiscible isotropic fluids (such as oil/water mixtures) result in round droplets of one fluid suspended in the other. Isotropic/nematic phase separation in TMV suspensions produces ellipsoidal droplets (Bernal and Fankuchen, 1941). The macroscopic rods observed in region 3 could be a single layer of a smectic phase of end-to-end aggregated TMV, or several layers of monodisperse TMV, coexisting with an isotropic background phase. Later we will see that in region 4 these rods evolve into a lamellar structure reminiscent of a smectic phase, but with key distinctions.

The rods are clearly dynamic structures with internal fluctuations. The rods are highly birefringent, whereas the platelike objects that also form in this region are not. It may be that these rods and plates are actually the same objects, only viewed from different perspectives. Three-dimensional reconstruction of these objects needs to be done to get more information about the relation between these two structures. There are several points of observation which support the idea that the rods and plates may be like objects. For example, it has been noted that within one sample, a range of rod sizes can exist. Smaller rods form out of the droplet structures first observed in region 2, and the larger macroscopic rods are the result of the coalescence of these subunits. Within a sample, it is generally the case that the rods are surrounded by other rods of roughly the same size. In some samples, the plates also appear in a range of sizes. The width of these plates and the length of rods in the vicinity of those plates seem to correspond in a given area of the sample. In some samples, the macroscopic rods appear to have a textured perimeter (Fig. 3 *d*). In such samples, the plates have a similar surface texture (Fig. 3 *e*).

Although the rods appear highly dynamic, the plates in most samples do not. In most samples, the plates seem to lie flat within the plane of observation. However, in some samples, the plates appear to be oriented at oblique angles to this plane. Differential interference microscopy is used at high magnification to enhance the contrast of our samples. By using differential interference microscopy and focusing through these oblique plate structures, fluctuations within a plate are made clearly visible.

Over time the macroscopic rods come together, in some samples forming very long structures that align with the

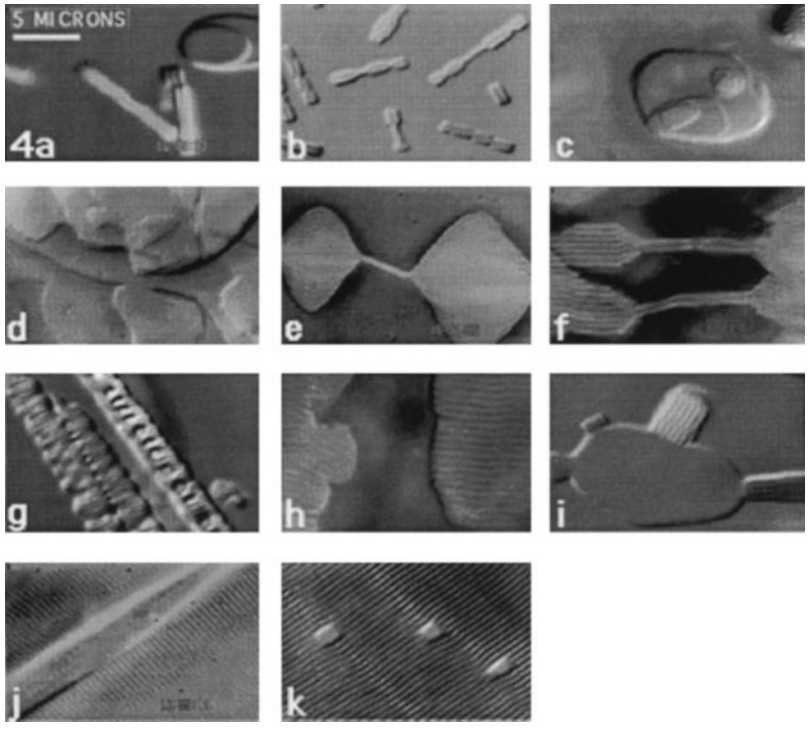

FIGURE 4 These samples correspond to behavior observed in region 4 of concentration space. Sample *a*: 130 mg/ml TMV; 5 mg/ml BSA. Stacking of rods and plates was observed. Sample *b*: 110 mg/ml TMV; 2.5 mg/ml PEO 100,000. This sample illustrates the formation of stacked rods from smaller subunits. (*Samples c* and *d*) 120 mg/ml TMV; 5 mg/ml PEO 100,000. Several stacked plates were observed (*c*), as was an overlapping texture of plates (*d*). (*Samples e*, *f*, and *g*) 96 mg/ml TMV; 10 mg/ml BSA. Several interesting structures were seen in this sample, including lamellar droplets connected by a birefringent strand (*e*). A similar side-by-side configuration of regions of lamellar phase (with more well-defined layers) connected by a few layers of lamellae was also observed (*f*). Several lamellar droplets have adhered, one on top of the other, to form a filament (*g*). (*Sample h*) 130 mg/ml TMV; 5 mg/ml BSA. This is an example of floating lamellar sheets, as described in the text. The periodicity of lamellar structures is ~0.75 μm. (*Sample i*) 120 mg/ml TMV; 5 mg/ml BSA. Lamellae appear to grow out of this plate. (*Sample j*) 130 mg/ml TMV; 2.5 mg/ml BSA. This sample exhibited curved domains of lamellar phase with a slightly lower periodicity than most of the other lamellar samples, ~0.66 μm. (*Sample k*) 120 mg/ml TMV; 5 mg/ml PEO 100,000. Extended lamellar phase with isotropic reservoirs or voids formed in this sample. The photograph of sample *k* was taken at the surface of the sample; all other photographs were taken within the bulk of the samples. Photographs are all high-magnification differential interference microscopy.

long axis perpendicular to the capillary walls, in the plane of observation. These rods can extend for hundreds of microns across the capillary (Fig. 3 *f*).

Plates are observed to stack, forming a series of steps. Rods are also seen stacked together. This defines the boundary between region 3 and region 4. In region 4, the TMV concentration falls within the isotropic-nematic coexistence region for the pure rod system. Again, macroscopic rod and plate structures form within this region, but unlike region 2, there are many more examples of stacking (Fig. 4, *a* and *b*).

The microscope used in this study has a depth of field of ~0.2 μm. An object's depth can be roughly measured by focusing through the object. In this way, measurements of the step size in a stack of plates give a value of ~3 μm. In a sample exhibiting such stacks of plates in the vicinity of a few macroscopic rods stacked together, the individual rods in a stack appear to have a thickness less than this, approximately a micron. It is clear that the relationship between these objects needs further study. We note that the point spread function of the microscope is highly anisotropic, with a resolution perpendicular to the image plane (*z* direction) three times less than the resolution in the image plane (*xy* direction). Thus a periodicity of ~0.7 μm, which is desirable in the image plane, may not be resolved if oriented perpendicular to the image plane.

Some samples exhibit individual rods stacking to form a filament-like structure. As mentioned previously, plates may stack on top of one another, forming a series of steps (Fig. 4 *c*). The plate structures can also combine to form an overlapping texture somewhat "melted" together, which can cover a large area of the sample (Fig. 4 *d*).

There are new structures that form in this region of phase space that exhibit a layered form not constructed of discrete macroscopic components. Ellipsoidal lamellar droplets with a central rod structure have also been observed (Fig. 4 *e*). The periodicity of the lamellar phase is ~0.75 μm. These droplets are dynamic, and the layers undulate and are not well defined. This structure is consistent with a smectic phase of TMV dimers, end-to-end aggregated. We never observed a lamellar structure with a periodicity of the monomer length of 300 nm. This seems strange, given that most of the TMV, in the absence of added depletant, is in the monomeric form. Perhaps the depletant induces dimerization of TMV, or alternatively, the longer dimers preferentially form lamellar phases. This lamellar phase may consist of layers of TMV rods, alternating with layers of depletant, as theoretically predicted (Koda et al., 1996) and

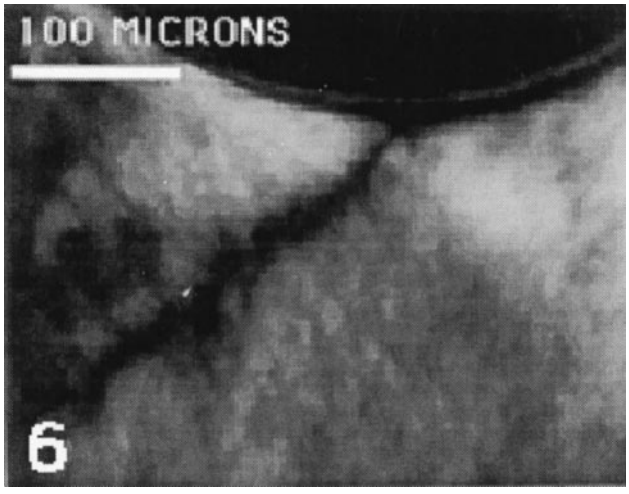

FIGURE 6 240 mg/ml TMV; 3 mg/ml PEO 100,000. A dense, disordered, birefringent gel-like phase was formed in region 6. This phase formed throughout the sample. The photograph is low-magnification standard polarization microscopy.

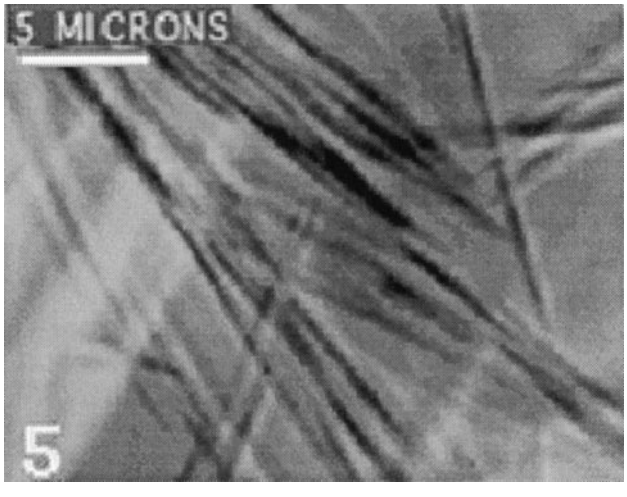

FIGURE 5 80 mg/ml TMV; 50 mg/ml BSA. A dense, static, highly birefringent precipitate with an isotropic liquid phase was formed in region 5. The photograph was taken within the bulk of the sample, using high-magnification differential interference microscopy.

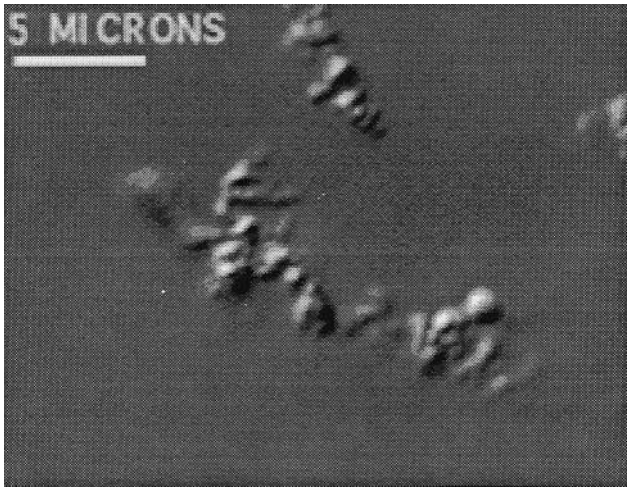

FIGURE 7 0.5 mg/ml TMV; 10 mg/ml PEG 8000; 0.5 M NaCl. The conditions of this sample correspond to those used in previous studies of virus precipitation (Leberman, 1966; Yamamoto et al., 1970). Such earlier work does not describe the morphology of the precipitated virus. This sample exhibits a dense, static precipitate. This photograph was taken within the bulk of the sample, using high-magnification differential interference microscopy.

recently observed in mixtures of the virus fd and PEO (Adams et al., manuscript submitted for publication).

These lamellar droplets are observed to attach to other like droplets. They may combine in a side-by-side configuration (droplets joined together by macroscopic rods; Fig. 4 *f*) or many may adhere, one on top of the other, to form a filament (Fig. 4 *g*).

A more stable layered structure, best described as floating lamellar sheets, confines fluctuations to individual layers. These sheets are observed both on the surface and in the bulk of the samples. The structure as a whole seems stable, with well-defined boundaries (Fig. 4 *h*). The size of the sheets varies. Samples exhibiting these lamellar objects also show structures in which lamellae seem to grow out of a plate (Fig. 4 *i*). This observation supports the idea that macroscopic rods and plates are the same structures, but have orthogonal orientations. The background phase for the above structures is an isotropic liquid.

One sample, very low in BSA concentration (2.5 mg/ml) and at the high end of TMV concentration (130 mg/ml) for region 4, does not have an isotropic liquid phase. The sample shows somewhat curved domains of lamellar phase, with the remaining portions of the sample birefringent (Fig. 4 *j*). This type of sample is less dynamic than the above examples of lamellar droplets and floating sheets. A corresponding sample mixed with PEO 100,000, however, did not exhibit curved domains as in the BSA sample. Rather, the sheets seem to come together, forming an extended lamellar structure. This extended lamellar phase was on the surfaces of one sample and showed regions that appeared to be either isotropic reservoirs or voids (Fig. 4 *k*).

In region 5 of the phase diagram, the TMV concentration matches that of region 4. PEO mixtures were not explored in this area of phase space; the concentration of PEO 100,000 was more limited (because of its solubility in the buffer) than in the case of the BSA. In some samples, the concentration of BSA is greatly increased, to ~50 mg/ml. A very dense, static, fibrous precipitate is observed (Fig. 5). The precipitate is highly birefringent and coexists with an isotropic liquid background phase.

In region 6, TMV is increased further, and the mixtures with low to moderate amounts of added BSA/PEO appear birefringent, but the precipitates are so dense that it is difficult to classify the behavior. At low magnification, the samples appear dense and disordered, forming a birefringent, gel-like state with no evident thermal fluctuations (Fig. 6).

Polymer size

As early as 1942, virus precipitation by the addition of polymer has been observed (Cohen, 1942; Leberman, 1966; Yamamoto et al., 1970). This method of virus isolation and purification is recognized to be a rod-polymer system that exhibits depletion flocculation (Lekkerkerker and Stroobants, 1994). The Leberman and Yamamoto studies do not describe the morphology of the precipitated virus. We therefore prepared a TMV sample with conditions similar to those used in those studies, to observe first-hand the structure of the precipitate. The precipitated virus appeared dense and static, a morphology most closely resembling the behavior seen in region 5 of sample space (Fig. 7). The work done by Cohen on TMV mixed with a variety of biopolymers (such as gelatin, gum, starch, and heparin) reported the formation of a needle-like paracrystalline precipitate (Cohen, 1942), which again seems consistent with region 5. The Cohen study uses polymers that are somewhat distinct from PEO because of surface charge. It was noted by certain groups (Leberman, 1966; Yamamoto et al., 1970) that the precipitation of the rods depends on the concentration of added polymer, the concentration of added salt, and the molecular weight of the polymer.

Theoretical and experimental studies of depletion interactions between two charged spherical colloids have been presented by Walz and are expected to be qualitatively similar to the case of charged rods experimentally studied here (Mahadevan, 1990; Walz and Sharma, 1994; Sober and Walz, 1995). The total potential of mean force between rods suspended in a polymer solution is a sum of an attractive potential caused by the depletion force (Lekkerkerker and Stroobants, 1994), and a repulsive potential arising from the electrostatic repulsion between the like-charged rods (Onsager, 1949; Odijk, 1986; Fraden et al., 1993). The range of the depletion attraction is the polymer diameter for the neutral PEO and on the order of the effective diameter for the charged BSA, and the depth of the attractive interaction is proportional to the number density of depletant. If the rods are sufficiently charged and strongly repel each other, then the rods will never come close enough to each other to exclude the polymer from the region between the rods, and thus will never feel the depletion force. Adding salt screens the electrostatic repulsion, and when the separation between rods is less than the polymer diameter, the depletion force will be felt. As a rough guide one can consider that the rod surfaces do not come closer than a separation equal to $D_{\text{eff}} - D = \xi$. In this case, if the polymer diameter $d < \xi$, then there will be phase separation at low concentrations of added polymer, whereas if $d > \xi$, phase separation can only occur (if at all) at high polymer concentrations.

We studied a limited number of samples of TMV mixed with other sizes of polymer, in the same buffer as before, and thus $\xi = 17$ nm. The polymer molecular weights and hydrodynamic diameters studied were PEG 8,000, $d = 5.2$ nm; PEG 12,000, $d = 7.0$ nm; PEG 35,000, $d = 12$ nm: PEO 600,000, $d = 56$ nm (Devanand and Selser, 1990). Although there were only a few samples of each, the distinct behavior makes for interesting comparison with the BSA, $d = 7.4$ nm and PEO 100,000, $d = 20$ nm mixtures.

For the polymers with hydrodynamic diameters $d < \xi$, that is PEG 8,000–35,000, we found that the added polymer had no effect on the phase behavior until the polymer concentration exceeded 100–150 mg/ml, at which point the suspension, at an initial virus concentration of 150 mg/ml,

formed a single phase, which was birefringent with a gel-like texture, similar to that observed in region 6 (Fig. 6) of the PEO 100,000/TMV mixtures. However, in the case of PEO 100,000/TMV mixtures, for which $d > \xi$, the gel state formed at low PEO concentrations of 5 mg/ml. More extreme was the demixing observed when low concentrations of 5 mg/ml PEO 600,000 were added to a TMV suspension of 140 mg/ml. We observed a birefringent, fibrous gel phase that separates from an isotropic liquid (and therefore low in rod concentration) background phase. When confined to a long, thin capillary, the gel contracts radially and expands longitudinally, producing a periodic buckling along the length of the tube. The diameter of PEO 600,000 is ~56 nm. At 140 mg/ml of TMV, the average surface-to-surface spacing between the rods is less than 50 nm. This implies that there is a large free energy cost in inserting the PEO in the TMV suspension.

We observed that the BSA and PEO 100,000 systems behaved very similarly, although the hydrodynamic radius of the PEO is 20 nm and that of BSA is 7.4 nm. Recent work of Wadu-Mesthrige et al. gives experimental evidence that distinguishes the TMV/BSA from the TMV/PEO system (Wadu-Mesthrige et al., 1996). This study indicates that BSA adsorbs onto the surface of the TMV rods. Given that BSA adsorbs onto TMV, bridging of TMV particles is likely (Russel et al., 1989). Although the mechanisms of attraction may differ in the two systems (adsorption effects versus depletion interaction), the range and magnitude of the attraction would be similar, and thus similar phenomenology could result.

Alternatively, it may be that some maximum concentration of added BSA may coat the TMV rods, and any BSA remaining free in solution would then act as a depletant (Lekkerkerker, University of Utrecht, Utrecht, the Netherlands, private communication). Further studies would need to be done to better distinguish between the roles of adsorption and depletion of the BSA/TMV system.

Previous work

D. L. D. Caspar, W. Phillips, and M. Cahoon (Caspar, Florida State University, private communication) studied TMV/PEG 6,000 mixtures to produce crystals for x-ray crystallography studies. Under conditions of PEG concentrations of 50 mg/ml, 100 mM Tris (pH 8; ionic strength 50 mM), and moderate TMV concentrations, colloidal crystalline hexagonal crystals were observed that were similar in appearance to those in Fig. 3 *c*. X-ray studies of these crystals revealed the TMV rods to be oriented perpendicular to the plane of the crystal, and to be hexagonally closed-packed in the plane of the crystal.

CONCLUSIONS

The observed behaviors of the TMV/PEO 100,000 mixtures are believed to be entropically driven. Adding PEO 100,000 to suspensions of TMV of 7 mM ionic strength induces flocculation of the TMV. Beginning with low concentration of TMV, we found that upon the addition of polymer the first order phase formed consisted of long rodlike drops of TMV (region 2). These drops did not resemble nematic droplets observed at zero polymer concentration, but rather appeared as single smectic or crystalline layers. Increasing polymer concentration led to formation of hexagonal domains (region 3), similar in appearance to crystals where the TMV molecules were hexagonally close-packed (Caspar, Florida State university, private communication). For higher initial TMV concentrations, lamellar structures with a periodicity of twice the monomeric TMV length were observed (region 4), and for high polymer and TMV concentrations a homogeneous, birefringent gel-like state was observed.

For polymers with diameters larger than the PEO 100,000, the polymer appears to be largely, if not completely, excluded from the TMV, and an isotropic phase is observed to be in coexistence with the TMV suspension. These are the conditions used in force balance measurements of biopolymers (Millman et al., 1984; Podgornik et al., 1996). For PEO diameters smaller than PEO 100,000, the addition of polymer has little effect, except at quite elevated polymer concentrations (100–150 mg/ml), at which time a dense, disordered precipitate is formed.

In the above TMV/polymer mixtures, the ionic strength was a constant value of 7 mM. We plan to do future experiments in which ionic strength will be varied, where it is expected that the behavior will be a function of ionic strength.

The entire phase behavior observed in the TMV/polymer mixtures is qualitatively consistent with theoretical models based on the depletion force, which arises from mixing spheres and rods, and from electrostatic repulsion between the like-charged rods. Further quantitative studies in monodisperse samples of fd virus are under way (Adams et al., manuscript submitted for publication).

We greatly appreciate the contributions of Zvonimir Dogic and acknowledge discussions with Henk Lekkerkerker.

We thank the National Science Foundation for financial support (grants DMR-9705336 and DMR-9415656).

REFERENCES

Asakura, S., and F. Oosawa. 1958. Interaction between particles suspended in solutions of macromolecules. *J. Polym. Sci.* 33:183–192.

Asherie, N., A. Lomakin, and G. B. Benedek. 1996. Phase diagram of colloidal solutions. *Phys. Rev. Lett.* 77:4832–4835.

Bernal, J. D., and I. Fankuchen. 1941. X-ray and crystallographic studies of plant virus. *J. Gen. Physiol.* 25:111–165.

Bolhuis, P., and D. Frenkel. 1994. Numerical study of the phase diagram of a mixture of spherical and rodlike colloids. *J. Chem. Phys*, 101: 9869–9875.

Cohen, S. 1942. The isolation and crystallization of plant viruses and other protein macro molecules by means of hydrophilic colloids. *J. Biol. Chem.* 144:353–363.

Cuneo, P., E. Magri, A. Verzola, and E. Grazi. 1992. "Macromolecular crowding" is a primary factor in the organization of the cytoskeleton. *Biochem. J.* 281:507–512.

Devanand, K., and J. C. Selser. 1990. Polyethylene oxide does not necessarily aggregate in water. *Nature.* 343:739–741.

Flory, P. J. 1978. Statistical thermodynamics of mixtures of rodlike particles. 5. Mixtures with random coils. *Macromolecules.* 11:1138–1141.

Forsyth, P. A., Jr., S. Marcelja, D. J. Mitchell, and B. W. Ninham. 1978. Ordering in colloidal systems. *Adv. Colloid Interface Sci.* 9:37–60.

Fraden, S. 1995. Phase transitions in colloidal suspensions of virus particles. *In* Observation, Prediction, and Simulation of Phase Transitions in Complex Fluids. M. Baus, L. F. Rull, and J. P. Ryckaert, editors. Kluwer Academic Publishers, Dordrecht, the Netherlands. 113–164.

Fraden, S., G. Maret, and D. L. D. Caspar. 1993. Angular correlations and the isotropic-nematic phase transition in suspensions of tobacco mosaic virus. *Phys. Rev. E.* 48:2816–2837.

Frenkel, D. 1991. Statistical mechanics of liquid crystals. *In* Liquids, Freezing, and Glass Transition. J. P. Hansen, D. Levesque, and J. Zinn-Justin, editors. North-Holland, Amsterdam. 689–762.

Frenkel, D. 1993. Order through disorder: entropy-driven phase transitions. *In* Proceedings of the Sitges Conference on Complex Liquids. L. Garrido, editor. Springer Verlag, New York. 137–148.

Gast, A. P., W. B. Russel, and C. K. Hall. 1986. An experimental and theoretical study of phase transitions in the polystyrene latex and hydroxyethylcellulose system. *J. Colloid Interface Sci.* 109:161–171.

Herzfeld, J. 1996. Entropically driven order in crowded solutions: from liquid crystals to cell biology. *Acc. Chem. Res.* 29:31–37.

Israelachvili, J. N., and B. W. Ninham. 1977. Intermolecular forces—the long and short of it. *J. Colloid Interface Sci.* 58:14–25.

Koda, T., M. Numajiri, and S. Ikeda. 1996. Smectic—a phase of a bidisperse system of parallel hard rods and hard spheres. *J. Phys. Soc. Jpn.* 65:3551–3556.

Leberman, R. 1966. The isolation of plant viruses by means of "simple" coacervates. *Virology.* 30:341–347.

Lekkerkerker, H. N. W., P. Buining, J. Buitenhuis, G. J. Vroege, and A. Stroobants. 1995. Liquid crystal phase transitions in dispersions of rodlike colloidal particles. *In* Observation, Prediction, and Simulation of Phase Transitions in Complex Fluids. M. Baus, L. F. Rull, and J. P. Ryckaert, editors. Kluwer Academic Publishers, Dordrecht, the Netherlands. 53–112.

Lekkerkerker, H. N. W., and A. Stroobants. 1994. Phase behaviour of rod-like colloid + flexible polymer mixtures. *Il Nuovo Cimento.* 16D: 949–962.

Mahadevan, H., and C. K. Hall. 1990. Statistical-mechanical model of protein precipitation by non-ionic polymer. *AIChE J.* 36:1517–1528.

Mao, Y., M. E. Cates, and H. N. W. Lekkerkerker. 1995. Depletion force in colloidal systems. *Physica A.* 222:10–24.

Meyer, R. B. 1990. Ordered phases in colloidal suspensions of tobacco mosaic virus. *In* Dynamics and Patterns in Complex Fluids. Springer-Verlag, New York. 62–73.

Millman, B. M., T. C. Irving, B. G. Nickel, and M. E. Loosley-Millman. 1984. Interrod forces in aqueous gels of tobacco mosaic virus. *Biophys. J.* 45:551–556.

Minton, A. P. 1995. Macromolecular crowding: a foreword. *Biophys. Chem.* 57:1–2.

Odijk, T. 1986. Theory of lyotropic polymer liquid crystals. *Macromolecules.* 19:2313–2329.

Onsager, L. 1949. The effects of shape on the interaction of colloidal particles. *Ann. N.Y. Acad. Sci.* 51:627–659.

Podgornik, R., H. H. Strey, K. Gawrisch, D. C. Rau, A. Rupprecht, and V. A. Parsegian. 1996. Bond orientational order, molecular motion, and free energy of high-density dna mesophases. *Proc. Natl. Acad. Sci. USA.* 93:4261–4266.

Poon, W. C. K. 1997. Crystallization of globular proteins. *Phys. Rev. E.* 55:3762–3764.

Rosenbaum, D., P. C. Zamora, and C. F. Zukoski. 1996. Phase behavior of small attractive colloidal particles. *Phys. Rev. Lett.* 76:150–153.

Russel, W. B., D. A. Saville, and W. R. Schowalter. 1989. Colloidal Dispersions. Cambridge University Press, Cambridge.

Semenov, A. N., and A. R. Khokhlov. 1988. Statistical physics of liquid-crystalline polymers. *Sov. Phys. Usp.* 31:988–1014.

Smits, C., B. van der Most, J. K. G. Dhont, and H. N. W. Lekkerkerker. 1992. Influence of non-adsorbing polymer on the formation of colloidal crystals. *Adv. Colloid Interface Sci.* 42:33–40.

Sober, D. L., and J. Y. Walz. 1995. Measurement of long range depletion energies between a colloidal particle and a flat surface in micellar solutions. *Langmuir.* 11:2352–2356.

Stroobants, A., H. N. W. Lekkerkerker, and T. Odijk. 1986. Effect of electrostatic interaction on the liquid crystal phase transition in solutions of rodlike polyelectrolytes. *Macromolecules.* 19:2232–2238.

Suzuki, A., M. Yamazaki, and T. Ito. 1989. Osmoelastic coupling in biological structures. *Biochemistry.* 28:6513–6518.

Ullmann, K., G. S. Ullmann, and G. D. J. Phillies. 1985. Critical probe study of a nonentangling macromolecule solution—bovine serum albumin: water. *J. Colloid Interface Sci.* 105:315–324.

Vroege, G. J., and H. N. W. Lekkerkerker. 1992. Phase transitions in lyotropic colloidal and polymer liquid crystals. *Rep. Prog. Phys.* 8: 1241–1309.

Vroege, G. J., and H. N. W. Lekkerkerker. 1993. Theory of the isotropic-nematic-nematic phase separation for a solution of bidisperse rodlike particles. *J. Phys. Chem.* 97:3601–3605.

Wadu-Mesthrige, K., P. Biswajit, W. M. McClain, and G. Liu. 1996. Disaggregation of tobacco mosaic virus by bovine serum albumin. *Langmuir.* 12:3511–3515.

Walter, H., and D. E. Brooks. 1995. Phase separation in cytoplasm, due to macromolecular crowding, is the basis for microcompartmentation. *FEBS Letts.* 361:135–139.

Walz, J. Y., and A. Sharma. 1994. Effect of long range interactions on the depletion force between colloidal particles. *J. Colloid Interface Sci.* 168:485–496.

Wang, J. H., F. Lonberg, X. Ao, and R. B. Meyer. 1994. Light scattering studies of a nematic to smectic-a phase transition in rigid rod polymer solutions. *In* Ordering in Macromolecular Systems. Springer-Verlag, New York. 171–179.

Warren, P. B. 1994. Depletion effect in a model lyotropic liquid crystal-theory. *J. Phys. I France.* 4:237–244.

Welch, G. R., and J. S. Clegg, editors. 1986. The Organization of Cell Metabolism. Plenum Press, New York.

Wetter, C. 1985. Die flussigkristalle des tabakmosaikvirus. *Biol. Unserer Zeit.* 3:81–89.

Yamamoto, K. R., B. M. Alberts, R. Bensinger, L. Lawhorne, and G. Treiber. 1970. Rapid bacteriophage sedimentation in the presence of polyethylene glycol and its application to large-scale virus purification. *Virology.* 40:734–744.